한국표면공학회지
J. Kor. Inst. Surf. Eng.
Vol. 36, No. 5, 2003.
<연구논문>

a-C:H Films Deposited in the Plasma of Surface Spark Discharge at Atmospheric Pressure. Part I: Experimental Investigation

Hui-Gon Chun[a*], K.V. Oskomov[b], N.S. Sochugov[b],
Jing-Hyuk Lee[a], Yong-Zoo You[a]

[a]School of Materials Science and Engineering, ReMM, University of Ulsan, Ulsan 680-749, Korea
[b]Institute of High Current Electronics SD RAS, 4 Akademichesky Ave., 634055 Tomsk, Russia

(Received 12 August 2003 ; accepted 30 September 2003)

Abstract

The aim of this work is the synthesis of a-C:H films from methane gas using surface spark discharge at the atmospheric pressure. Properties of these films have been investigated as functions of energy W delivered per a methane molecule in the discharge. The method enables the coatings to be deposited with high growth rates (up to 100 μm/hour) onto large-area substrates. It is shown that the films consist of spherical granules with diameter of 20~50 nm formed in the spark channel and then deposited onto the substrate. The best film characteristics such as minimum hydrogen-to-carbon atoms ratio H/C=0.69, maximum hardness H_V=3 GPa, the most dense packing of the granules and highest scratch resistance has been obtained under the condition of highest energy W of 40 eV. The deposited a-C:H coatings were found to be more soft and hydrogenated compared to the diamond-like hydrogenated (a-C:H) films which obtained by traditional plasma-enhanced chemical vapor deposition methods at low pressure (<10 Torr). Nevertheless, these coatings can be potentially used for scratch protection of soft plastic materials since they are of an order harder than plastics but still transparent (the absorption coefficient is about 10^4 ~10^5 m^{-1}). At the same time the proposed method for fast deposition of a-C:H films makes this process less expensive compared to the conventional techniques. This advantage can widen the application field of these films substantially.

Keywords : a-C:H films, methane, atmospheric pressure, spark discharge

1. INTRODUCTION

Amorphous hydrogenated carbon (a-C:H) films combine a set of unique properties, which are high hardness (up to 30 GPa) and partial transmittance in the IR and visible ranges. These films can be used as protective and wear-resistant coatings for optical components made of soft dielectric materials. A rather rich variety of techniques for vacuum plasma deposition of a-C:H films is now available[1]. However, these techniques are limited in use because of their low productivity and high cost of final product. Hence, the attempts to produce a-C:H films by electric discharges at atmospheric pressure seem to be worth-while.

Currently, studies are also been made to use a barrier discharge at atmospheric pressure to produce a-C:H films that can be referred to as polymer-like because of their properties[2]. Obviously, the reason for the polymer-like nature of these films is insufficient destruction of hydrocarbon molecules in the barrier discharge plasma resulting in high hydrogen concentrations in the coatings. In this paper we suggest to use a surface spark discharge on a dielectric in methane gas at atmospheric pressure for a-C:H film deposition. This type of discharge consists of multiple single spark discharges, just as a barrier discharge consists of multiple micro-discharges. It is known that the energy delivered into the spark discharge channel is orders of magnitude higher (up to 100 J/cm^3)[3] than that delivered into a micro discharge in the case of a barrier discharge (10 μJ/cm^3)[4]. This would result in more efficient methane destruction in the plasma and lowering of hydrogen percentage in the coating layers. As a consequence, a-C:H films obtained by a surface spark discharge should be

*Corresponding author. E-mail : hgchun@mail.ulsan.ac.kr

closer to diamond-like coatings in their properties in comparison with the a-C:H films obtained by a barrier discharge. Besides the simplicity of this type of discharge that can be realized without complicated vacuum equipment, it is attractive because of possibility of fast deposition of a-C:H films on large-area low-melting-point substrates. However, no systematic data are now available on the structure and properties of such films. Thus, the goal of this work was to examine these a-C:H coatings deposited under various experimental conditions.

2. EXPERIMENTAL

For experiments on a-C:H film deposition in a surface spark discharge we used a chamber with dimensions of $200 \times 200 \times 10$ mm^3 presented schematically in Fig. 1. Glass substrates with dimensions of $90 \times 120 \times 2$ mm^3 (2) were placed on the metal bottom of the chamber (1). The chamber was filled with methane gas at atmospheric pressure. Two parallel 40-mm long electrodes (3 and 4) were placed at 0.3~0.5-mm away from the glass surface and 15-mm apart from each other. One electrode was grounded (4), and to the other electrode (3) the bipolar sinusoidal high-voltage pulses with a pulse repetition rate of 1 kHz, amplitude of 16 kV and width of approximately 100 μs were applied (Fig. 2(a)). The gap breakdown corresponded in time to the second half-wave maximum of a high-voltage pulse (see voltage drop in marked region on Fig. 2(a)) and occurred as a single spark discharge with a current width of up to 50 ns and amplitude up to 400 A (5) (Fig. 2(b)). The single spark discharge parameters were determined by the value of the storage capacitor (6) installed in parallel with the discharge gap. The

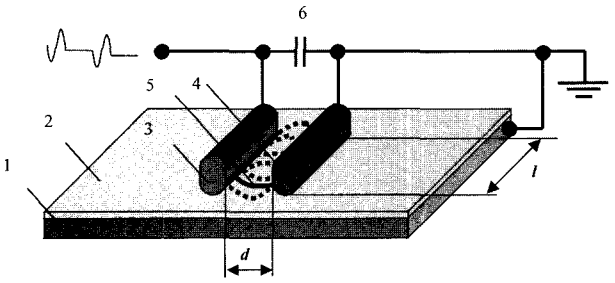

Fig. 1. Schematic drawing of the operating chamber for a-C:H film deposition in surface spark discharge: 1- base of the chamber (initiating electrode), 2- substrate, 3- high-voltage electrode, 4- grounded electrode, 5- single spark discharge, 6- storage capacitor.

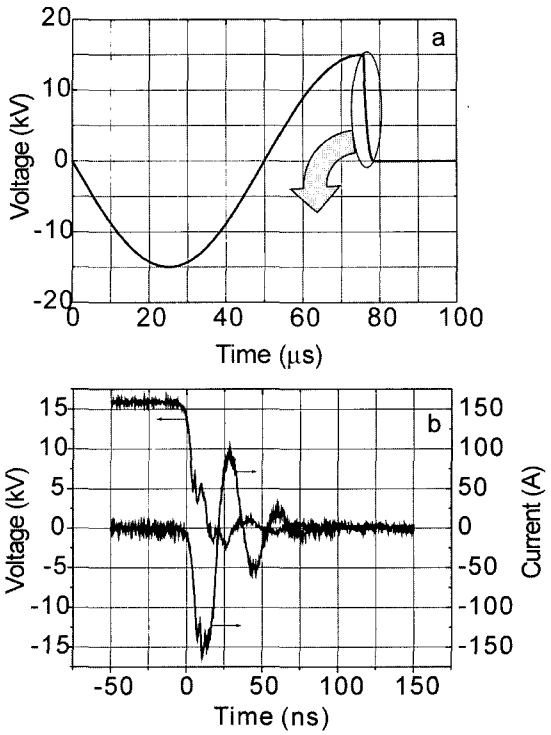

Fig. 2. Oscillogram of voltage applied to the high-voltage electrode. Voltage drop (marked by arrow) corresponds to gap breakdown by single surface spark discharge (a). Voltage and current oscillograms of a single surface spark discharge in methane (for the capacitor C = 100 pF) (b).

chamber bottom served as an initiating electrode and was placed under the ground potential that resulted in a gap breakdown voltage decrease and localization of single spark discharges near the dielectric surface. By fitting the optimum electrode forms and as a result of precise control of the distance between the electrodes and the glass surface, the probability of gap breakdown was equal at all places along the electrodes. Therefore, spark discharges and the a-C:H film formed uniformly cover the whole dielectric surface between the electrodes. Using extended (up to 1 m) electrodes and scanning of the substrate, one can coat large-area substrates by the a-C:H film quite uniformly.

The energy delivered into a spark was determined by integration of the current and discharge voltage oscillograms recorded with a low-inductive shunt, capacity divider and Tektronix TDS 3000 oscilloscope (Tektronix, USA) with a ratio error of ±10-15%. The thickness of the coatings and their refractive index at $\lambda = 630$ nm were determined with an MII-4 interference microscope (LOMO, Russia). The absorption coefficient of the a-C:H films at $\lambda = 530$ nm and their optical gap width were determined with an SF-46 spec-

trophotometer (LOMO, Russia).

A quantitative analysis of the chemical composition of the produced coatings was carried out with the use of absorption IR spectroscopy and computational analysis by a method similar to that described in[5]. But, in contrast to it, our method described below, was based on comparison with standards (polyethylene, polypropylene and polystyrene films).

It is known, that absorption frequency and strength of single C-H bond in its stretch vibration region are independent on chemical and phase composition of whole coating. These quantities depend only on state of carbon atom in the bond, namely, type of its hybridization (sp^3, sp^2 or sp) and hydrocarbon group (CH_3, CH_2 or CH)[5]. Concentration of any sort of C-H bonds mentioned above is proportional to absorption integral[6]:

$$n_i^{CH} = A_i \alpha_i(k)/k \, dk, \quad (1)$$

where n_i is concentration of certain sort of C-H bonds, $\alpha_i(k)$ is absorption coefficient, k is wavenumber and A_i is experimental coefficient.

Taking into account that dependence of the absorption coefficient on the wavenumber $\alpha_i(k)$ for any bond is symmetric function (Lorentzian)[6], one can rewrite the formula (1) as follows:

$$n_i^{CH} = A_i S_i/k_i, \quad (2)$$

where S_i is an area under $\alpha_i(k)$ curve and k_i is a characteristic vibration wavenumber for certain sort of C-H bonds. Now the coefficients A_i for each type of C-H bonds can be determined from IR spectra of standards after their decomposition into subbands. Subsequently concentrations n_i^{CH} for all kinds of C-H groups in deposited films were determined after decomposition of their IR spectra into subbands. Then *H/C* ratio can be determined as

$$H/C = \frac{m_C \cdot \sum_i n_i^{CH}}{\rho - m_H \cdot \sum_i n_i^{CH}}, \quad (3)$$

where ρ is the film density, m_C and m_H are masses of carbon and hydrogen atoms. Here concentrations of all detected kinds of C-H bonds must be summarized. It should be noted that IR analysis allows to detect only chemically bonded hydrogen, so its content on the film can be higher due to physisorption.

Also hydrocarbon groups ratio (CH_3 : CH_2 : CH) and C-C bonds types ratio (sp^3/sp^2) can be obtained[5]. The latter ratio includes only hydrogen-bonded carbon atoms, so it is valid in the case of high *H/C*, when almost all carbon atoms are hydrogen-bonded and detected by IR analysis, i.e. in all cases being under consideration in this paper. IR spectra were recording using IKS-29 IR spectrophotometer (LOMO, Russia), then decomposed into subbands using Origin™ software and analyzed according to data on IR spectra of organic species[7]. The films deposited for IR analysis were usually 5 to 10 μm thick.

For investigation of the surface morphology, Solver P47 atomic-force microscope (NT-MDT, Zelenograd, Russia) was used. A semi-contact imaging regime was applied using a whisker-type silicon cantilever. The a-C:H films deposited onto the glass were investigated; in all cases the coating thickness was about 2 μm. For statistical purposes 5 images in different locations were acquired for each sample, and then the most typical of them were presented in this paper. To investigate the hardness and elastic modulus of the *a-C:H* coating surface layer, a NanoTest 600 nanoindenter (MicroMaterials, Wrexam, Great Britain) was used. Films of about 2 μm thick deposited onto glass were analyzed. The maximum load was 0.5 mN; the indenter penetration depth did not exceed 5~10% of the film thickness. Dependences of the penetration depth of the diamond Berkovich indenter into the coating on the applied force in the loading and unloading stages were analyzed by the Oliver and Pharr method[8]. The final values of the hardness and elastic modulus were obtained by averaging the results of ten measurements. Film density was measured by the flotation method in mixtures of CCl_4 and ethanol. Density of these mixtures can be varied from 0.8 to 1.6 g/cm^3.

3. RESULTS AND DISCUSSION

Figure 3 presents the surface images of the a-C:H films deposited in a surface spark atmospheric pressure discharge obtained by the atomic-force microscope. The conclusion can be made that the a-C:H films consist of spherical granules with a diameter of approximately 20~50 nm. The fact that the height of granules in the given images is much less than their diameter can be explained by the existence of shadow zones, which the cantilever tip does not penetrate in. The reason is the fact that cantilever radius of curvature and vertex angle are 20 nm and 20 degrees, respectively, which is close to the characteristic dimensions of the objects under investigation[9]. It is also should be noted that the a-C:H coatings obtained

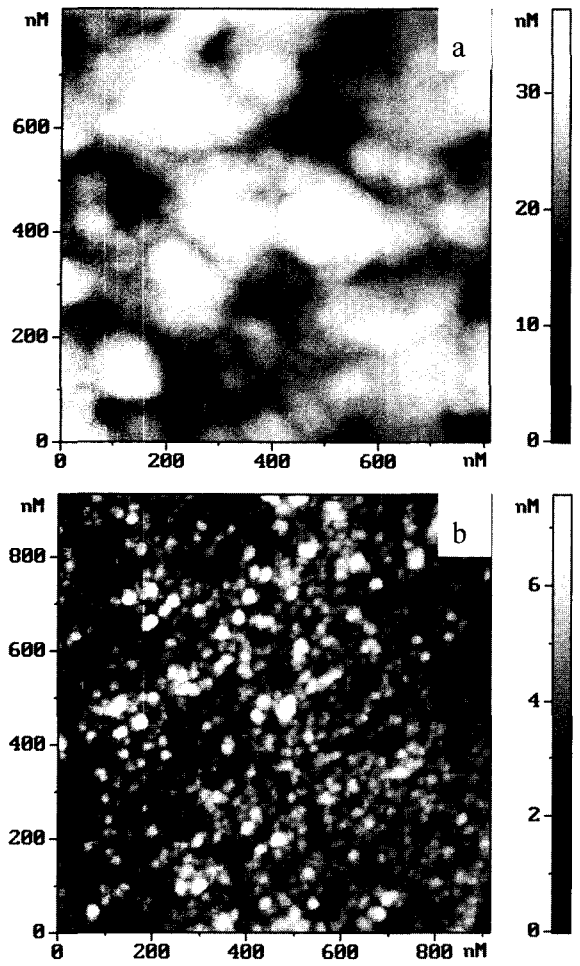

Fig. 3. Surface morphology of the a-C:H films obtained with an atomic-force microscope: a) sample SD1, b) sample SD5 (see Tables 1 and 2).

at higher energy delivered in a spark (SD5, Fig. 3(b)) are characterized by more dense packing of granules, different from the sample SD1 (Fig. 3(a)). In the former case the granules are not agglomerated, unlike in the latter one. It is shown in the following that this type of coating (SD5) is marked by a greater hardness.

It is well-known that optical and mechanical properties of a-C:H films are determined by the ratio of sp^3- and sp^2-hybridized carbon atoms as well as by the percentage of hydrogen atoms in a coating[10]. These characteristics in our case should be determined by the gas phase chemistry in the spark channel and, hence, by the specific energy delivered per methane molecule W:

$$W = \frac{1}{n_0}\int_0^{\tau} w(t)dt \qquad (4)$$

where $w(t)$ is the volumetric power density delivered in the spark at the stage of current flowing, τ is the duration of a single spark discharge, and $n_0 = 2.688 \times 10^{19}$ cm^{-3}. In turn, power density can be determined after processing the current and discharge voltage oscillograms if the spark channel widening dynamics are known:

$$w(t) = \frac{I(t)U(t)}{\pi \cdot r^2(t) \cdot L}, \qquad (5)$$

where L is the spark channel length, $I(t)$ is the discharge current, $U(t)$ is the discharge voltage, and $r(t)$ is the radius of the current flow region. It was considered in formula (4) that concentration of particles in the channel during current flow did not change. In reality, the processes of methane dissociation into hydrocarbon radicals and atomic hydrogen and their recombination to form stable products (acetylene, ethylene, ethane and molecular hydrogen) are actively going on even at this stage. Because the cross-section of different processes of electron interaction with hydrocarbon radicals is much larger than that with atomic or molecular hydrogen[11], it can be considered that, during the current flow through the spark channel, energy is transferred to heavier particles. In turn, as will be shown in the following, according to the law of conservation of matter, total concentration of hydrocarbon radicals and molecules remains within the limit of 50 to 100% of $n_0 = 2.688 \times 10^{19}$ cm^{-3}. Hence, to approximate the energy contributed per gas molecule, one can approximately use formula (4). The main problem arising in the process of experimental determination of W is a complicated behavior of the radius of the current flow region $r(t)$. Usual photography cannot clarify this question. That is why we use the average value of $\langle r(t) \rangle = 10^{-2}$ cm obtained by Ryzhov and collaborators[12] from a computer simulation of the spark development in methane under similar conditions (gap breakdown voltage U = 12 kV, length d = 1 cm, and approximate peak current is I = 300 A).

Figure 2(b) presents characteristic oscillograms of current and voltage for a single spark discharge. There are damped current and voltage oscillations in the spark; however, the main energy is contributed in 20~30 ns that correspond to the width of the first half-wave of the current. The only parameter that was changed in the course of the experiments was the value of the storage capacitor C that determined the discharge characteristics. Table 1 presents the values of the breakdown voltage U_0, peak current I_{max}, single spark discharge duration τ (the width of the first half-wave of the current) and specific energy

Table 1. Characteristics of single spark discharge

Sample	C (pF)	U_0 (kV)	I_{max} (A)	τ (ns)	E_0 (mJ)	E (mJ)	W (eV)
SD1	100	16±2	127±13	26	13±3	16±3	8.0±1.6
SD2	150	16±2	162±16	26	19±4	21±4	10.2±2.0
SD3	200	16±2	280±28	27	26±5	25±5	12.3±2.5
SD4	250	16±2	333±33	30	32±6	32±6	15.9±3.2
SD5	300	16±2	269±27	37	38±8	41±8	20.0±4.0

C = storage capacitance, U_0 = breakdown voltage, I_{max} = peak discharge current, τ = discharge duration, $\AA_0$ = energy stored in capacitor, $\AA$ = energy delivered in discharge, W = energy delivered per methane molecule

W delivered per methane molecule versus the storage capacitor C. The values of W were calculated using formulas (4) and (5); the channel radius in formula (5) was considered to be constant and equal to the average radius $\langle r(t)\rangle = 10^{-2}$ cm. Moreover, Table 1 presents the values of the energy stored in the storage capacitor E_0 and the energy extracted in the spark E (obtained by integration of the oscillograms). These values coincide within the limits of experimental measurement error.

Properties of the a-C:H films deposited in the surface spark discharge versus energy delivered per methane molecule are plotted in Fig. 4, and some coating properties are also presented in Table 2. As was already noted, properties of the a-C:H films are determined by the ratios of sp^3/sp^2 and H/C. Study of the coatings by IR spectroscopy (Fig. 5) have shown that the population of tetrahedrically-bonded carbon

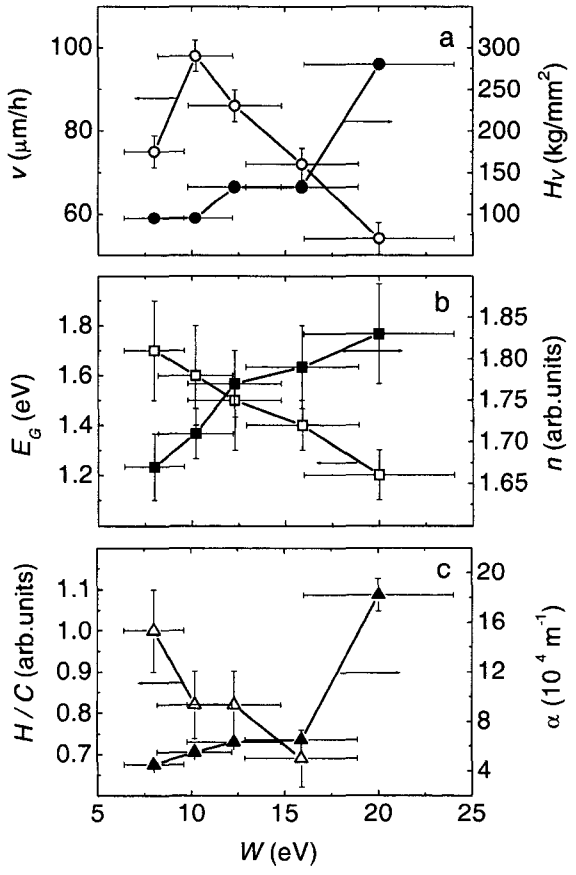

Fig. 4. Experimental dependences of the rate of growth v (○), hardness H_V (●), optical gap width E_G (□), refractive index n (λ = 630 nm) (■), atomic hydrogen to carbon ratio H/C (△) and absorption coefficient α (λ = 530 nm) (▲) of the a-C:H coatings on the specific energy W delivered per methane molecule.

Table 2. Characteristics of a-C:H films

Sample	Film Density (g/cm³)	Hardness (GPa)	Elastic modulus (GPa)
SD1	1.2	0.95±0.02	9.1±0.1
SD2	1.2	0.95±0.02	9.1±0.1
SD3	1.2	1.25±0.04	9.5±0.1
SD4	1.2	1.25±0.04	9.5±0.1
SD5	1.3	2.80±0.07	17.3±0.4

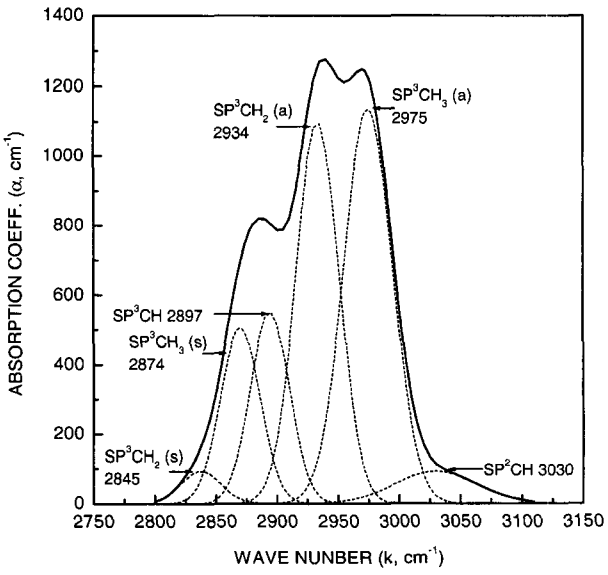

Fig. 5. IR absorption from C-H bonds stretch vibration for the coating deposited from CH_4 in surface discharge and its decomposition into subbands.

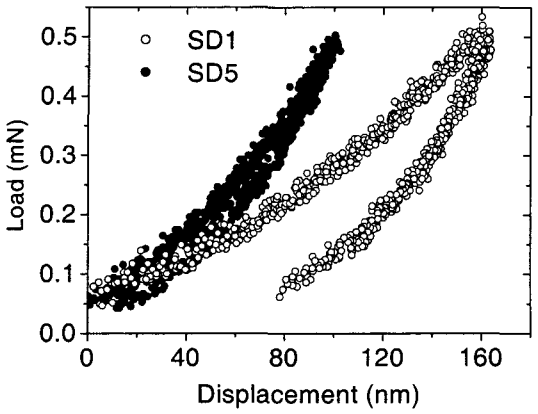

Fig. 6. Indenter displacement versus load for the hardness and elasticity modulus measurements for the samples SD1 and SD5 (see Tables 1 and 2).

atoms was more than 90% and did not depend on energy delivered for all sputtering regimes considered here. The share of *CH* groups in the film is maximum (about 60%) and grows with increasing *W*. More exact information concerning the ratio of hydrocarbon groups was not obtained. Hydrogen concentration in the coating decreases monotonically from *H/C* = 1.025 to *H/C* = 0.69 as *W* increases from 8 to 20 eV (Fig. 4(c)). At the same time, the coating hardness H_V (Fig. 4(a)), the refractive index n at λ = 630 nm (fig. 4(b)) and the absorption coefficient α at λ = 530 nm (Fig. 4(c)) all increase, while the width of the optical gap E_G (Fig. 4(b)) decreases. Similar behavior of the main properties is characteristic of all a-C:H films and reflects a transition from polymer-like to diamond-like structure[13]. It is should be noted that the increase in the films hardness can be caused by both lowering of hydrogen percentage and densification of the granules with *W* increase.

It is necessary to note sufficient effect of the elastic recovery of the indentations. From Fig. 6 it follows that the indentation is recovers by 80~90% in depth for sample SD5. This effect is common for all amorphous hydrocarbon coatings for which nano-indentation may be the only method of studying their mechanical properties[14]. The a-C:H films studied in this work are an order of magnitude harder than soft polymeric materials (e.g. for PMMA the Knoop hardness is 0.2 GPa)[11]; moreover, they have high transparency in the visible range (Fig. 4(c)). Hence, a given a-C:H film can be used as protective coating on optical components made of soft polymeric materials (polycarbonate, PMMA, etc.).

It is obvious from Fig. 4 that the main characteristics of the a-C:H films correlate with the *H/C* ratio of the films and are changed monotonically. It can be supposed that the decrease of hydrogen in a film with an increase in *W* is related to more complete methane decomposition in the spark. The only exception is the non-monotonic behavior of the coating rate of growth $v(W)$ (Fig. 4(a)) that can be explained only after a quantitative evaluation of the concentrations of methane dissociation products in the discharge. Hence, changes in the characteristics of the a-C:H films obtained in a surface spark discharge taking place with the rise of specific energy delivered per methane molecule are explained most likely by changing chemical composition of the gas phase, although it should be theoretically improved yet.

4. CONCLUSIONS

The high cubic density (30~100 J/cm^3) of the delivered energy in case of the surface spark discharge in methane promotes formation of a-C:H films with high growth rates (50~100 μm/hour). The main characteristics of the a-C:H films depend on the specific energy delivered per methane molecule, and as the energy increases, the coating properties shift from polymer-like to diamond-like a-C:H films. The coatings obtained (H_V = 1~3 GPa) are harder by an order of magnitude than polymer-like hydrocarbon films and polymer materials; moreover, they have high transparency in the visible range (α is about 5×10^4 m^{-1} for λ = 530 nm). Therefore, the a-C:H films can be used as protective coatings on optical components made of soft polymeric materials (polycarbonate, PMMA, etc.). Besides high a-C:H film growth rate, it is necessary as well to note the energetic efficiency and scalability of the given method of obtaining coatings that makes it technologically attractive.

ACKNOWLEDGEMENTS

This work was supported in part by the Korea Science and Engineering Foundation (KOSEF) through the Research Center for Machine Parts and Materials Processing (ReMM) at the University of Ulsan, Korea.

REFERENCES

1. J. Robertson, Surf. Coat. Technol. 50 (1992) 185.
2. Schwarz and I. Salge, *Proc. 11th Int. Symp. Plasma*

Chemistry, Ed. J.E. Harry (Loughborough, England, 1993) 1071.
3. V. Kozyrev, Yu. D. Korolev and K. A. Tinchurin, Fizika Plazmy 14 (1988) 1003 (in Russian).
4. V. G. Samoylovich, V. I. Gibalov and K. V. Kozlov, *Physical Chemistry of the Barrier Discharge*, Eds. V. I. Gorshkov and S. D. Razumovsky (Moscow State University Publishing, Moscow, 1989) (in Russian).
5. J. Zou, K. Schmidt, J. Appl. Phys. 67 (1989) 484.
6. M. Cardona, Phys. Stat. Sol. B 118 (1983) 463.
7. L. J. Bellamy, *The Infrared Spectra of Complex Molecules* (Methuen & Co. LTD, London, 1957).
8. W. Oliver and G. Pharr, J. Mater. Res. 7 (1992) 1564.
9. A. A. Buharaev, I. V. Berdunov and D. V. Ovchinnikov, Mikroelektronika 26 (1997) 163 (in Russian).
10. M. Ham and K. A. Lou, J. Vac. Sci. Technol. A 8 (1990) 2143.
11. *Physical Quantities: Handbook*, Eds. I. S. Grigoriev and E. Z. Meylihov (Energoatomizdat, Moscow, 1991).
12. A.V. Kirikov, V.V. Ryzhov and A.I. Suslov, *Proc. 14th Int. Symp. Plasma Chemistry*, Ed. M. Hrabovsky (Prague, Czech Republic, 1999) 921.
13. S. Kumar, P. N. Dixit, D. Sarangi and R. Bhattacharyya, Appl. Phys. Lett. 69 (1996) 49.
14. S. Logothetidis and C. Charitidis, Thin Solid Films 208 (1999) 353.